Vehicle System Dynamics, 33 (2000), pp. 29–48 0042-3114/00/3301-029$15.00

The Force-Angle Measure of Tipover Stability Margin for Mobile Manipulators

EVANGELOS PAPADOPOULOS * and DANIEL A. REY [1]

SUMMARY

Mobile manipulators operating in field environments will be required to apply large forces, or manipulate large loads, and to perform such tasks on uneven terrain which may cause the system to approach, or reach, a dangerous tipover instability. To avoid tipover in an automatic system, or to provide a human operator with an indication of proximity to tipover, it is necessary to define a measure of available stability margin. This work presents a new tipover stability measure (the Force-Angle stability measure) which has a simple geometric interpretation, is easily computed, and is sensitive to changes in Center of Mass height. The proposed metric is applicable to systems subject to inertial and external forces, operating over even or uneven terrains. Requirements for computation and implementation of the measure are described, and several different categories of application of the measure are presented along with useful normalizations. Performance of the Force-Angle measure is demonstrated and compared with that of other stability margin measures using a forestry vehicle simulation. Results show the importance of considering both center-of-mass height and system heaviness, and confirm the effectiveness of the Force-Angle measure in monitoring the tipover stability margin.

1. INTRODUCTION

Mobile machines equipped with manipulator arms and controlled by on-board human operators are commonplace systems in the construction, mining, and forestry industries, see for example Figure 1. When these systems exert large forces, move heavy payloads, or operate over very uneven or sloped terrain, tipover instabilities may occur which endanger the operator, risk damaging the machine, and reduce productivity. With the introduction of computer control in mobile manipulator systems (i.e., a supervisory control system) the safety and productivity of these mobile manipulators can be improved by automatic detection and prevention of tipover instabilities. In order to accomplish this, an appropriate measure of the *tipover stability margin* must be defined. Teleoperated or fully autonomous mobile manipulators operating in field environments (as proposed by

* Corresponding author. National Technical University of Athens, Dept. of Mechanical Engineering, 9 Heroon Polytechniou, Zografou, 15773 Athens, Greece. Fax: +301-772-1455; E-mail: egpapado@central.ntua.gr
[1] Department of Mechanical Engineering and Centre for Intelligent Machines, McGill University, Montreal, Que., Canada H3A 2A7.

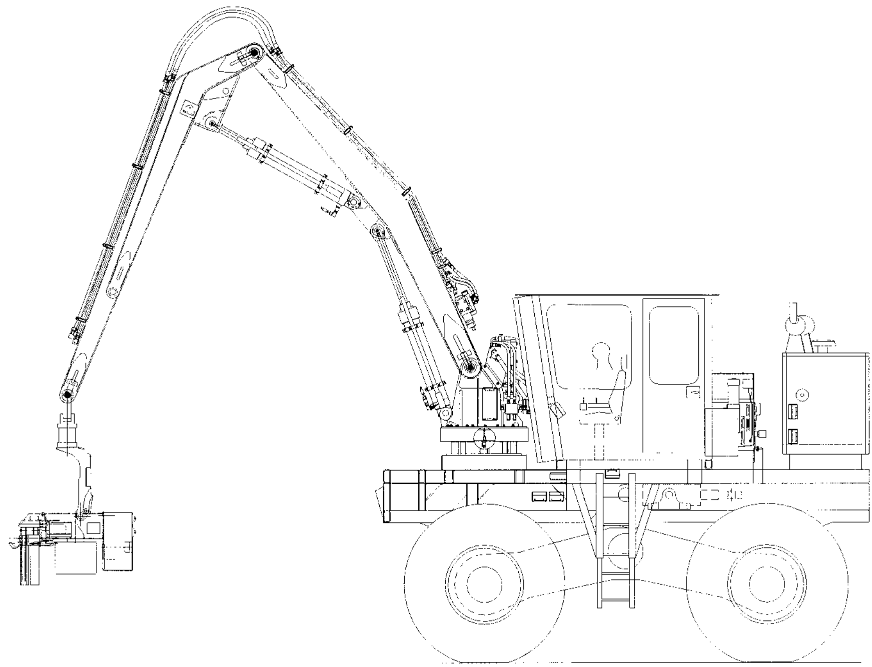

Fig. 1. Example mobile manipulator.

the nuclear, military and aerospace industries) would also benefit by a similar monitoring of the tipover stability margin.

Related work by the vehicular research community has focused on characterizing the lateral rollover propensity of a vehicle [1–3]. While the proposed static characterizations of machine lateral stability are not appropriate as instantaneous measures of a vehicle's stability, they do highlight the importance of considering vehicle center-of-mass (C.M.) height and system mass (i.e., heaviness). Attempts by the robotics research community to solve elements of the motion planning problem for mobile manipulators gave rise to various stability constraint definitions [4–6]. Li and Frank used a stability constraint to solve the inverse kinematic solution for a planar, redundant mobile manipulator. Dubowsky and Vance used their stability constraint to bound manipulator joint velocities in solving for the time optimal motion of a manipulator arm on a free base (i.e., a non-fixed base which is free to tipover). Shiller and Gwo used their stability constraint in solving for the time optimal motion of a mobile robot traveling over sloped terrain. While these stability constraints do not provide an instantaneous measure of the stability margin, one could consider the degree to which they are satisfied in order to obtain a measure of the stability margin. However, all of the resulting stability measures would not be top-heavy sensitive as they only consider the moments about the tipover axes, or the magnitudes of the normal ground reaction forces.

Several researchers examined more directly the question of how one should define the instantaneous measure of stability margin for a mobile manipulator. McGhee proposed the use of the shortest horizontal distance between the center-of-mass and the support pattern boundary projected onto a horizontal plane [7,8]. This measure was refined by Song and later by Sugano, yet it remains insensitive to what we shall refer to as topheaviness (introduced in Section 3.1) and their measure is only an approximation for systems on uneven terrain [9,10]. Sreenivasan and Wilcox improved on the minimum distance measure by considering the minimum distance from each contact point[2] to the net force vector, thereby eliminating the need for a projection plane and making the measure exact [11]. However, this measure fails in the presence of angular loads and also does not take into consideration topheaviness. Davidson and Schweitzer also extended the work of McGhee, this time using screw mechanics to provide a measure which eliminates the need for a projection plane while allowing for angular loads [12]. They recognized however that their measure is not sensitive to topheaviness. Messuri and Klein proposed the use of the minimum work required to bring the static vehicle to the point of tipover. This measure termed the Energy stability margin measure has the property of being sensitive to center-of-mass height [13]. However, this approach requires the assumption of constant load magnitude and direction throughout the tipover motion. To capture manipulator inertial and external loads, Ghasempoor and Sepheri extended this energy-based approach by introducing an inclined equilibrium plane for each tipover axis [14]. This measure, however, does not take into account the dynamics of the base platform and computation of the work to tipover requires the non-physical assumption of constant load magnitude and direction throughout the tipover motion.

This work describes the *Force-Angle* tipover stability measure which has a simple geometrical interpretation, is easily computed and implemented, remains sensitive to topheaviness and is applicable to the general case of systems operating over uneven terrain, or of systems subject to inertial and external forces. The simple nature of the proposed measure, its comprehensiveness, and the fact that it does not require any integration make it advantageous to previously proposed measures.

Requirements for computation and implementation of the measure are described, and several different categories of application of the measure are presented along with useful normalizations. Performance of the stability margin measure is demonstrated and compared with that of other stability margin measures using a forestry vehicle simulation. Results show the importance of considering both center-of-mass height and system heaviness, and confirm the effectiveness of the Force-Angle measure in monitoring the tipover stability margin.

[2] To apply this measure to the full 3-dimensional case, one should use the tipover axis rather than the contact point.

2. BACKGROUND

In determining the tipover stability margin of a ground vehicle system, one is necessarily concerned with the stability of the central body which generally provides mobility, i.e., the vehicle body or base. It is assumed in this work that the vehicle body is nominally in contact with the ground, as would be the case if mobility is provided via wheels, tracks, alternating (statically stable) legged support, or a combination thereof. A tipover or rollover instability occurs when a nominally upright vehicle body undergoes a rotation which results in a reduction of the number of ground contact points such that all remaining points lie on a single line (the tipover axis). Mobility control is then lost, and finally, if the situation is not reversed, the vehicle is overturned.

A low center-of-mass height is always desirable from a tipover stability point-of-view, heaviness on the other hand is stabilizing at low velocities, and destabilizing at high velocities. In this work we are concerned with low velocity systems possibly exerting large forces on the environment, hence, heaviness will be considered to have a stabilizing effect.

3. FORCE-ANGLE STABILITY MEASURE

To help frame the discussion of the general form of the Force-Angle stability measure we first present a planar example which highlights its simple graphical nature.

3.1. Planar Example

Shown in Figure 2 is a two contact point planar system whose system Center of Mass (C.M.) is subject to a net force $\mathbf{f}_r$ which is the sum of all forces acting on the

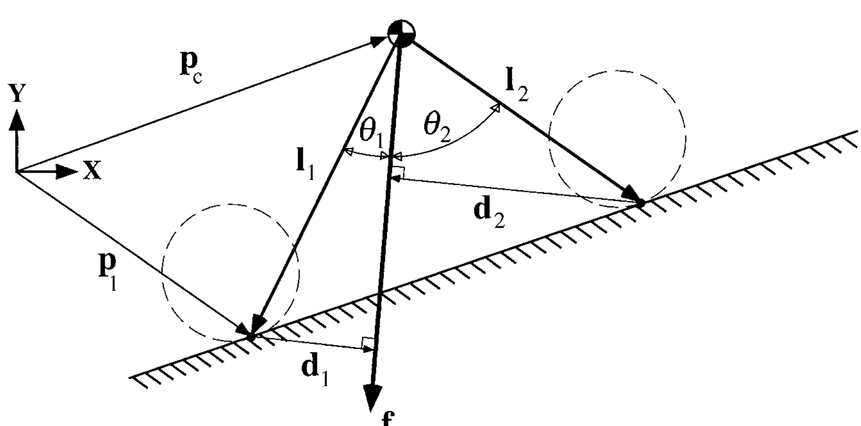

Fig. 2. Planar Force-Angle stability measure.

mobile system except the supporting reaction forces (which do not contribute to a tipover motion instability). This force vector subtends two angles, θ_1 and θ_2, with the two tipover axis normals $\mathbf{l}_1$ and $\mathbf{l}_2$, and acts along a line which is at a distance of $\|\mathbf{d}_1\|$ and $\|\mathbf{d}_2\|$ respectively from the two tipover axes. The Force-Angle stability measure, β, is given by the minimum of the product of θ_i, $\|\mathbf{d}_i\|$, and $\|\mathbf{f}_r\|$. Thus we have

$$\beta = \theta_i \cdot \|\boldsymbol{d}_i\| \cdot \|\boldsymbol{f}_r\| \tag{1}$$

Critical tipover stability occurs when β goes to zero, i.e., when any θ_i becomes zero, or when any $\|\mathbf{d}_i\|$, or the force $\mathbf{f}_r$ become zero. The angle θ_i becomes zero when the net force is coplanar with one of the tipover axes $\mathbf{l}_i$, and this is the typical manner in which a tipover instability occurs. If $\mathbf{f}_r$ lies outside the cone described by $\mathbf{l}_1$ and $\mathbf{l}_2$, the angle becomes negative and tipover is in progress. The distance $\|\mathbf{d}_i\|$ becomes zero as the net force is coplanar with one of the tipover axes, or, as the system C.M. approaches one of the tipover axes. This latter case is less frequent, requiring a system with reconfigurable legged support or that a very large payload be held far below the support plane. Note that these two geometric parameters, θ_i and $\|\mathbf{d}_i\|$, together characterize the tipover stability margin of the system. The angle θ_i captures the effect of topheaviness (where we use the term topheaviness to describe a change in the system C.M. height along the net force vector $\mathbf{f}_r$) and the distance $\|\mathbf{d}_i\|$ captures the effect of changes in the moment contribution of the net force. Finally, weighing by the magnitude of $\mathbf{f}_r$ is used to provide heaviness sensitivity since when $\mathbf{f}_r$ approaches zero, even the smallest disturbance may topple the vehicle.

For a mobile system which is capable of varying its C.M. height, or of carrying and manipulating a variable payload, it is important that the tipover stability margin be sensitive to the reduced stability associated with an increase in the C.M. height along $\mathbf{f}_r$. For the Force-Angle stability measure, this is illustrated in Figure 3 where an *increase* in C.M. height clearly results in a *smaller* minimum angle and therefore, a reduced β. Note that measures which use only a ratio of the normal forces at the ground contact points or a measure of the minimum moment exerted by $\mathbf{f}_r$ with respect to the tipover axes, are not sensitive to stability margin changes associated with changes in the system C.M. height.

3.2. General Form

Geometry. Of all the vehicle contact points with the ground, it is only necessary to consider those outermost points which form a *convex* support polygon when projected onto a horizontal plane. These points will simply be referred to as the ground contact points. Let $\mathbf{p}_i$ represent the instantaneous inertial location of the ith ground contact point, defined as

$$\boldsymbol{p}_i = [\, p_x \; p_y \; p_z \,]_i^T \quad i = \{1, \ldots, n\} \tag{2}$$

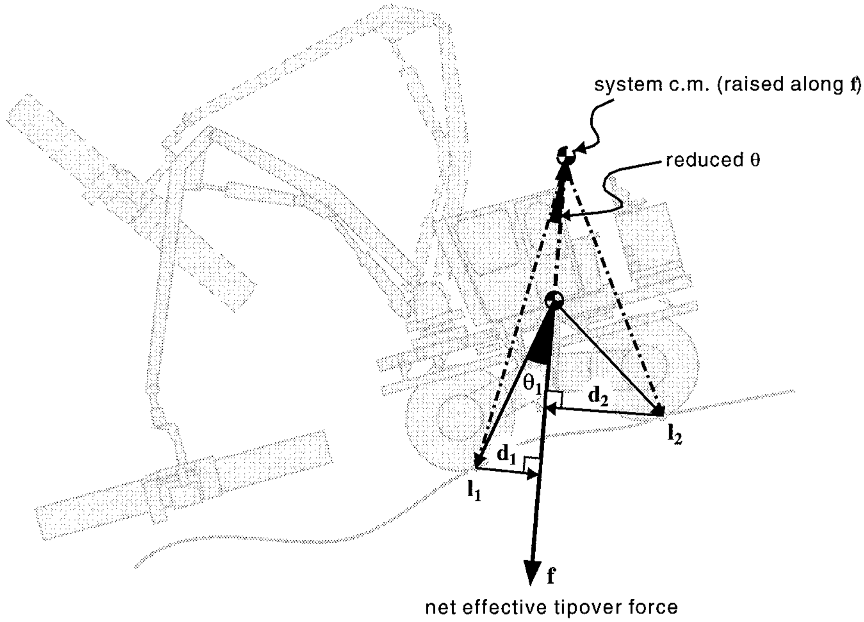

Fig. 3. Effect of center-of-mass height.

and let $\mathbf{p}_c$ represent the instantaneous inertial location of the *system* C.M.

$$\boldsymbol{p}_c = \frac{\sum_j \boldsymbol{p}_{mass_j} m_j}{m_{tot}} \tag{3}$$

where $\mathbf{p}_{\mathrm{mass}}$ is the inertial location of the system's jth lumped mass and m_{tot} is the total system mass. Note that for clarity all vectors are expressed in an inertial frame but that use of a reference frame located at the system C.M. would result in additional simplifications as $\mathbf{p}_c$ would be a zero vector.

Also note that the use of the *system* C.M. here is in contrast to the original Force-Angle measure presented in [15] where the *vehicle* C.M. was used. Use of the system C.M. improves the Force-Angle measure by making it sensitive to changes in *system* C.M. height, thereby fully capturing the susceptibility to tipover of the entire system. For mobile systems which do not have a manipulator, or for systems for which the manipulator and payload masses are negligible with respect to the vehicle mass, computation of the Force-Angle measure can be accelerated by using the vehicle C.M. rather than the system C.M.

For a consistent formulation, the $\mathbf{p}_i$ are numbered in ascending order following a right-hand rule convention where the thumb is directed downwards along the gravity vector, i.e., the ground contact points are numbered in clockwise order when viewed from above. The lines which join the ground contact points are the candidate tipover mode axes, $\mathbf{a}_i$, and the set of these lines will be referred to as the *support pattern*. Note that the support pattern does not need to belong to a plane, and that the Force-Angle measure can be applied to mobile manipulators on arbitrarily uneven terrain. The ith tipover mode axis is given by

$$\boldsymbol{a}_i = \boldsymbol{p}_{i+1} - \boldsymbol{p}_i \quad i = \{1, \ldots, n-1\} \tag{4}$$

$$\boldsymbol{a}_n = \boldsymbol{p}_l - \boldsymbol{p}_n \tag{5}$$

as shown in Figure 4. The ground contact point numbering convention was required in order to obtain a set of tipover axes whose directions all coincide with that of *stabilizing* moments. For the simple case of a planar system like that of Figure 2 we would have $\mathbf{a}_1 = [0\ 0\ \text{-}1]^T$, and $\mathbf{a}_2 = [0\ 0\ 1]^T$, i.e. the axes are parallel to the plane normal.

A natural (i.e., untripped) tipover of the vehicle will always occur about a tipover mode axis $\mathbf{a}_i$. A tripped tipover of the vehicle occurs when one of the ground contact points encounters an obstacle or a sudden change in the ground conditions. In a tripped tipover the vehicle undergoes a rotation about an axis which is some linear combination of the tipover mode axes associated with the single remaining ground contact point. In a tripped instability the Force-Angle

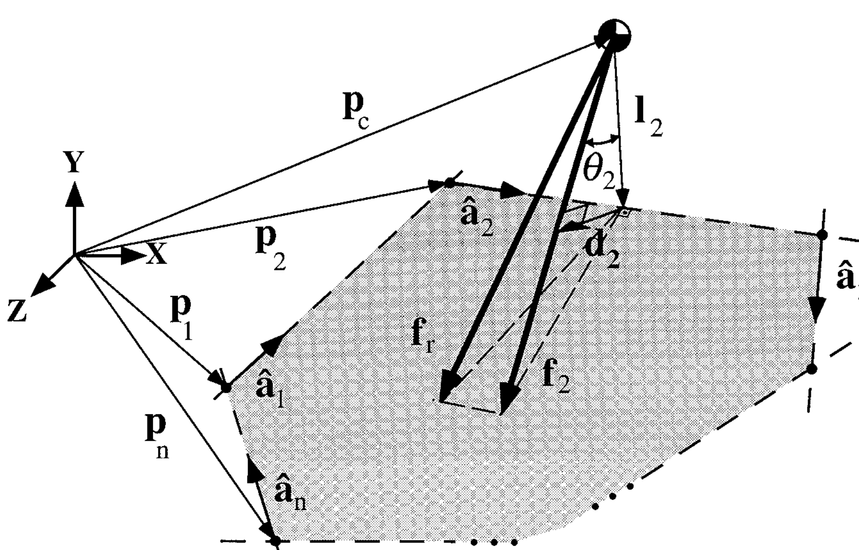

Fig. 4. 3D Force-Angle stability measure.

stability measure will go to zero and then become negative for each contributing tipover mode axis so that it is not required to identify the exact tipover mode axis.

Letting $\hat{\mathbf{a}} = \mathbf{a}/\|\mathbf{a}\|$, the tipover axis normals $\mathbf{l}_i$ which pass through the system C.M. are simply given by subtracting from $(\mathbf{p}_{i+1} - \mathbf{p}_c)$ that portion which lies along $\hat{\mathbf{a}}_i$, i.e.,

$$\boldsymbol{l}_i = \left(1 - \hat{\boldsymbol{a}}_i \hat{\boldsymbol{a}}_i^T\right)(\boldsymbol{p}_{i+1} - \boldsymbol{p}_c) \tag{6}$$

where $\mathbf{1}$ is the 3×3 identity matrix.

Dynamics. From Newtonian principles we have the following dynamic equilibrium of forces for overall system

$$\Sigma \boldsymbol{f}_{inertial} = \Sigma \boldsymbol{f}_{grav} + \Sigma \boldsymbol{f}_{ee} + \Sigma \boldsymbol{f}_{support} + \Sigma \boldsymbol{f}_{dist} \tag{7}$$

where $\mathbf{f}_{\text{inertial}}$ are the inertial forces, $\mathbf{f}_{\text{grav}}$ are the gravitational loads, $\mathbf{f}_{\text{ee}}$ are the loads transmitted by the manipulator end-effector to the system (due to end-effector loading and end-effector reaction forces), $\mathbf{f}_{\text{support}}$ are the reaction forces of the vehicle support system, and $\mathbf{f}_{\text{dist}}$ are any other external disturbance forces acting directly on the system (e.g., forces due to a trailer implement). Note that in the absence of independent inertias between the vehicle body and the ground, $\mathbf{f}_{\text{support}}$ is equal to the ground reaction forces.

The net force acting on the system C.M. that would participate in a tipover instability, $\mathbf{f}_r$, is thus given by

$$\boldsymbol{f}_r = \Sigma \boldsymbol{f}_{grav} + \Sigma \boldsymbol{f}_{ee} + \Sigma \boldsymbol{f}_{support} + \Sigma \boldsymbol{f}_{dist} - \Sigma \boldsymbol{f}_{inertial} \tag{8}$$

$$= -\Sigma \boldsymbol{f}_{support} \tag{9}$$

For the case of a static vehicle subject only to gravitational loading the above reduces to $\mathbf{f}_r = \Sigma \mathbf{f}_{\text{grav}} = m_{tot}\mathbf{g}$ where $\mathbf{g}$ is the gravitational acceleration.

Similarly, the net moment $\mathbf{n}_r$ acting about the system C.M. is given by

$$\boldsymbol{n}_r = \Sigma \boldsymbol{n}_{ee} + \Sigma \boldsymbol{n}_{dist} - \Sigma \boldsymbol{n}_{inertial} \tag{10}$$

$$= -\Sigma \boldsymbol{n}_{support} \tag{11}$$

where $\mathbf{n}_{\text{ee}}$, $\mathbf{n}_{\text{dist}}$, and $\mathbf{n}_{\text{support}}$ include both applied external moments or reaction moments, and the moment arm contribution of $\mathbf{f}_{\text{ee}}$, $\mathbf{f}_{\text{dist}}$, and $\mathbf{f}_{\text{support}}$ respectively about the system C.M.

For a given tipover axis $\hat{\mathbf{a}}_i$ we are only concerned with those components of $\mathbf{f}_r$ and $\mathbf{n}_r$ which act *about* the tipover axis, so we let

$$\boldsymbol{f}_i = \left(\mathbf{1} - \hat{\boldsymbol{a}}_i \hat{\boldsymbol{a}}_i^T\right) \boldsymbol{f}_r \tag{12}$$

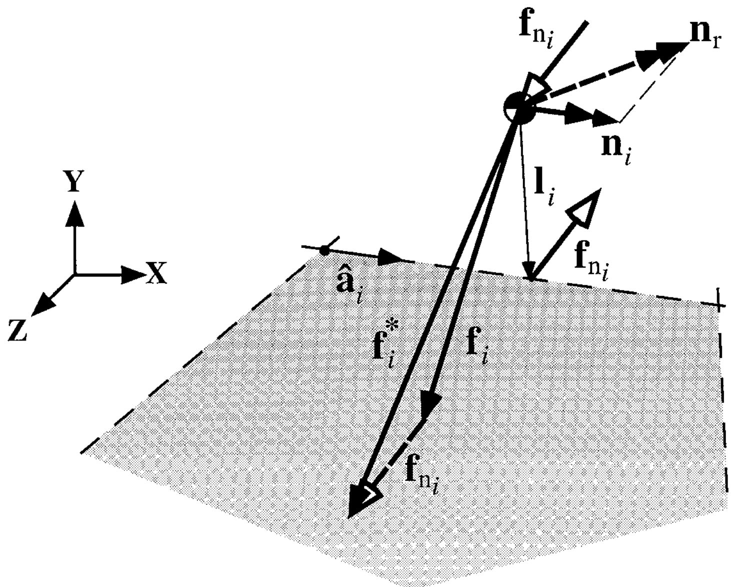

Fig. 5. Use of equivalent force couple to replace moment at C.M.

and

$$\boldsymbol{n}_i = \left(\hat{\boldsymbol{a}}_i \hat{\boldsymbol{a}}_i^T\right) \boldsymbol{n}_r \tag{13}$$

Angular Loads. Since the Force-Angle stability measure is based on the computation of the angle between the net *force* vector and each of the tipover axis normals, it is necessary to replace the moment $\mathbf{n}_i$ with an equivalent force couple $\boldsymbol{f}_{n_i}$ for each tipover axis. The equivalent force couple must necessarily lie in the plane normal to the moment $\mathbf{n}_i$. The most judicious choice of the infinite possible force couple locations and directions in this plane, is that pair of minimum magnitude where one member of the couple passes through the system C.M. and the other through the line of the tipover axis.

As shown in Figure 5, the member of the force couple acting on the center-of-mass is then given by

$$\boldsymbol{f}_{n_i} = \frac{\hat{\boldsymbol{l}}_i \times \boldsymbol{n}_i}{\|\boldsymbol{l}_i\|} \tag{14}$$

where $\hat{\mathbf{l}} = \mathbf{l}/\|\mathbf{l}\|$. Finally, the effective net force vector for the ith tipover axis which captures the effects of both force and angular loads, $\mathbf{f}_i^*$, is thus given by

$$\boldsymbol{f}_i^* = \boldsymbol{f}_i + \frac{\hat{\boldsymbol{l}}_i \times \boldsymbol{n}_i}{\|\boldsymbol{l}_i\|} \tag{15}$$

It is the angle which this vector makes with the ith tipover axis normal $\mathbf{l}_i$ that will be used to compute the Force-Angle stability margin measure as we show next.

Force-Angle Stability Measure. Since $\mathbf{l}_i$ and $\mathbf{f}_i^*$ lie in a plane normal to tipover axis $\mathbf{a}_i$, the set of minimum length vectors from the tipover axes $\mathbf{a}_i$ to $\mathbf{f}_i^*$ are simply found by adding the projection of $\mathbf{l}_i$ on $\mathbf{f}_i^*$ to negative $\mathbf{l}_i$, i.e.,

$$\boldsymbol{d}_i = -\boldsymbol{l}_i + \left(\boldsymbol{l}_i^T \cdot \hat{\boldsymbol{f}}_i^*\right) \hat{\boldsymbol{f}}_i^* \quad i = \{1, \ldots, n\} \tag{16}$$

where $\hat{\mathbf{f}}_i^*$ denotes the unit vector along $\mathbf{f}_i^*$, i.e. $\hat{\mathbf{f}} = \mathbf{f}^* / \|\mathbf{f}^*\|$ The candidate angles for the Force-Angle stability measure are then simply given by

$$\theta_i = \sigma_i \cos^{-1}\left(\hat{\boldsymbol{f}}_i^* . \hat{\boldsymbol{l}}_i\right) \quad i = \{1, \ldots, n\} \tag{17}$$

where $0 \leq \theta_i / \sigma_i \leq \pi$. The appropriate sign of the θ_i angle measures associated with each tipover axis is introduced by σ_i and is determined by establishing whether the effective net force vector $\mathbf{f}_i^*$ is directed inside or outside the support pattern. Since the tipover axis normals are directed *from* the system C.M. to the tipover axes, and the direction of the tipover axes correspond to that of a stabilizing moment, we have that the projection of the cross-product between the effective net force vector $\mathbf{f}_i^*$ and the tipover axis normal $\mathbf{l}_i$ onto the tipover axis $\mathbf{a}_i$ is positive when the net force vector is directed inside the support pattern and negative otherwise. Thus,

$$\sigma_i = \begin{cases} +1 & \left(\hat{\boldsymbol{f}}_i^* \times \hat{\boldsymbol{l}}_i\right) \cdot \hat{\boldsymbol{a}} > \mathbf{0} \\ -1 & \text{otherwise} \end{cases} \quad \text{where } i = \{1, \ldots, n\} \tag{18}$$

The Force-Angle stability measure β is then simply given by

$$\beta = \min\left(\theta_i \cdot \|\boldsymbol{d}_i\| \cdot \|\boldsymbol{f}_i^*\|\right) \quad i = \{1, \ldots, n\} \tag{19}$$

Eq. (18) reveals that computing the Force-Angle stability margin measure β requires computing distances $\mathbf{d}_i$ using Eq. (12), angles θ_i using Eq. (17), and effective net force vectors $\mathbf{f}_i^*$ using Eq. (15), before determining the minimum product over the set of n tipover axes. Note that this definition of the stability margin not only gives an instantaneous measure of the tipover stability margin of the system, but also identifies the currently probable tipover axis. The magnitude of a positive β indicates the tipover stability margin of a stable system. Critical tipover stability occurs when $\beta = 0$. Negative values of β indicate that a tipover instability is in progress.

While this single measure can be used to describe the global tipover stability margin of the system, it is often advantageous to monitor the tipover stability margin measure associated with *each* of the tipover axes, e.g., for use in a display system for a human operated or teleoperated machine. To track the Force-Angle stability measures associated with the ith tipover axis one need simply use

$$\beta_i = \theta_i \cdot \|\boldsymbol{d}_i\| \cdot \|\boldsymbol{f}_i^*\| \tag{20}$$

3.3. Requirements

To compute the Force-Angle stability measure one must have knowledge of the location of the ground contact points of the vehicle relative to the system C.M. location. This is required to define the support pattern of the system. In order to be able to compute the location of the system C.M., one requires knowledge of the mass of the different principal system components and knowledge of the manipulator joint angles. In order to determine the net force and moment acting on the system C.M., it is sufficient to know the forces and moments exerted at the support points, as demonstrated by Eqs. (9) and (11). Alternatively, one can make use of knowledge of the external forces and moments acting on the vehicle, and knowledge of the vehicle linear and angular accelerations as described by Eqs. (8) and (10). All of these elements are readily available in any dynamic system simulation, and are all measurable quantities on a real system equipped with an appropriate sensor suite.

It is important to note that the Force-Angle stability margin measure does not require distinct knowledge of the gravitational loads on the system as does the Energy stability margin measure in its computation of the instantaneous equilibrium planes associated with each tipover axis [14]. This can have a significant impact on the sensor requirements for a real time monitoring implementation of the measure.

4. APPLICATIONS AND NORMALIZATION

4.1. Application Levels

Depending on the particular application of the Force-Angle stability measure, various normalizations are appropriate. Three levels of application for such a stability measure are identified here:

i) tipover stability margin monitoring for a *particular* mobile manipulator in operation or simulation,

ii) tipover stability characterization for comparing various machines in a given *weight / size class* or *application class* (e.g., micro-rovers or forestry vehicles),

iii) tipover stability characterization for comparing various machines belonging to different classes.

The level 1 application class is the principal target application for a stability margin measure such as the Force-Angle measure. It includes off-line simulation (for path planning and design optimization), real-time simulation (for operator training simulators), and real-time monitoring (for system/operator early warning, and for tipover prediction and prevention). Although tipover prediction and prevention methods remain an open topic for future research and are not directly addressed in this paper, a few preliminary observations can be made. One possible technique for tipover prediction is to use the gradient of the Force-Angle stability margin to compute a time to zero intercept of the Force-Angle measure. When the time to intercept is below a given threshold a tipover prevention mechanism could be initiated. Possible prevention methods include alerting the system operator to the danger of tipover and displaying a recommended recovery input. For an automated system the tipover prevention procedure could include an automated motion slow down and reversal, or a more sophisticated recovery algorithm based on the possible use of a system dynamics model.

4.2. Normalizations

For the level 1 application class, when the Force-Angle stability measure is applied to a particular mobile manipulator, one should normalize the stability measure by its nominal value in order to better condition the computational problem and to facilitate interpretation of the measure by a human operator or teleoperator if present, i.e.,

$$\hat{\beta}_i = \frac{\beta_i}{\beta_{nom}} \tag{21}$$

where β_{nom} is the nominal Force-Angle stability margin measure for the system on a level surface with the arm in its home position

For the level 2 case, one should consider using both the unnormalized Force-Angle stability measure, and the measure normalized by the nominal or maximum operating loads (inertial and external). While each of these measures predicts the same critical tipover stability point, together they provide a more revealing profile of system stability than a single characterization. For the level 3 case, where the machines belong to different classes, one must normalize by the nominal or maximum operating loads for a meaningful comparison.

5. EXAMPLE

The Force-Angle stability measure was implemented in a planar simulation of a mobile manipulator with fundamental characteristics similar to that of the forestry vehicle of Figure 1. The five body system consists of a principal vehicle body, a pair of pneumatic tires, a two degree-of-freedom revolute joint manipulator with rigid links, and a rigidly attached end-effector or tool. The longitudinal plane model captures inertial effects, external loading effects, tire slip and compliance.

Manipulator masses are assumed lumped at the joints. Key system parameters are listed in Table 1.

The seven system generalized coordinates include the three vehicle inertial pose coordinates, i.e., vehicle C.M. position (x_v, y_v), and vehicle pitch angle (θ_z), the two wheel angular positions (θ_i), and the two manipulator joint angles (ϑ_i):

$$\boldsymbol{q} = [\boldsymbol{q}_v | \boldsymbol{q}_w | \boldsymbol{q}_m]^T = [x_v, y_v, \theta_z | \theta_1, \theta_2 | \vartheta_1, \vartheta_2]^T \tag{22}$$

The system equations of the motion can be shown to be of the form

$$\boldsymbol{I}(\boldsymbol{q})\ddot{\boldsymbol{q}} + \boldsymbol{c}(\boldsymbol{q},\dot{\boldsymbol{q}}) + \gamma(\boldsymbol{q}) = \tau + \phi(\boldsymbol{q},\dot{\boldsymbol{q}}) \tag{23}$$

where the $\mathbf{I}$, $\mathbf{c}$, and $\boldsymbol{\gamma}$ are the inertia, velocity-dependent, and gravity tensors respectively, $\boldsymbol{\tau}$ are the input generalized forces, and $\boldsymbol{\phi}$ are the generalized external loads. The input force vector is of the form,

$$\tau = [\mathbf{0}^T | \tau_w^T | \tau_m^T]^T \tag{24}$$

where both $\boldsymbol{\tau}_w$ and $\boldsymbol{\tau}_m$ are determined using simple PD regulation about a desired vehicle trajectory and desired joint trajectories respectively. The external load vector $\boldsymbol{\phi}$ is given by the sum of the ground forces and moments acting on the system and the prescribed end-effector loads. No other external loads are assumed to be acting on the system. The longitudinal ground forces are determined using a Karnopp slipstick friction model [16,17]. The tire model accounts for the special cases of wheel hop or lift-off, locked wheels, backsliding, and reverse direction motion. The normal ground forces are prescribed at each tire contact patch by a first order spring-damper tire compliance model. The net force and moment vectors $\boldsymbol{f}_r$ and $\boldsymbol{n}_r$ acting on the system C.M. are computed using Eqs. (9) and (11).

Table 1. System parameters.

	Mass [kg]	Length [m]	Mom. of inertia [kgm^2]
vehicle	10,000	-	10,000
link 1	500	3.5	500
link 2	500	3.5	500
tool	1000	-	4000
	vehicle C.M. position [m]		$\mathbf{p}_v = [0.00, 0, 0.00]^T$
	front wheel hub position [m]		$\mathbf{p}_1 = [1.50, 0, -0.25]^T$
	rear wheel hub position [m]		$\mathbf{p}_2 = [-0.50, 0, -0.25]^T$
	manipulator base position [m]		$\mathbf{p}_b = [0.50, 0, 0.00]^T$
	undeformed tire radii [m]		$r_{\text{und}} = 0.65$
	nominal joint angles		$\mathbf{q}_m = [120°, -150°]^T$
	nom. sys. cm. position [m]		$\mathbf{p}_c = [0.13, 0, 0.30]^T$
	nominal θ_i (see Eq. (17))		$\theta_i = [53.0°, 45.8°]$

5.1. Sample Task

The sample task used here to demonstrate an evolution of the Force-Angle stability measure has four principal phases: i) the system is at rest, holding its position on an inclined surface of 5°, ii) the manipulator is commanded to reach forward and downward, iii) a heavy object (750 kg) is picked-up, and iv) the arm over-extends forward while carrying the object and a tipover instability is initiated. These different principal phases of the sample task sequence are illustrated in the schematic of Figure 6.

To highlight the sensitivity of the Force-Angle measure to variations in base loading and center-of-mass height, two additional cases are studied where the *same* sample task is performed. In one case the vehicle is initially loaded with 7500 kg (e.g., of logs or construction material) and the resulting increase in vehicle center-of-mass height is 0.5 m. In the second hypothetical case the center-of-mass is again raised by 0.5 m but without an associated increase in the mass of the base. The three cases are thus labeled: A) unloaded vehicle, B) loaded vehicle with raised center-of-mass, and C) unloaded vehicle with raised center-of-mass.

6. RESULTS

Presented in Figure 7 is the time history of the normalized Force-Angle stability margin measure, $\hat{\beta}$, for all three study cases. For reference purposes, the manipu-

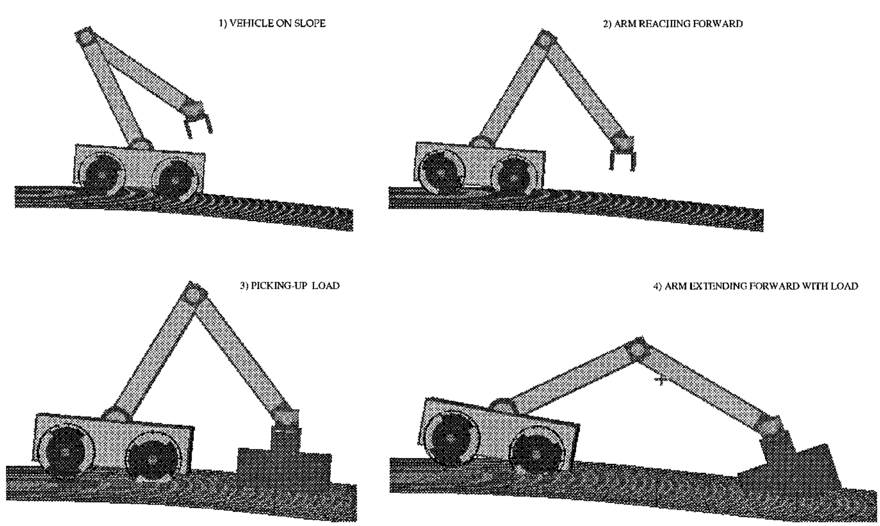

Fig. 6. Schematic of sample task sequence.

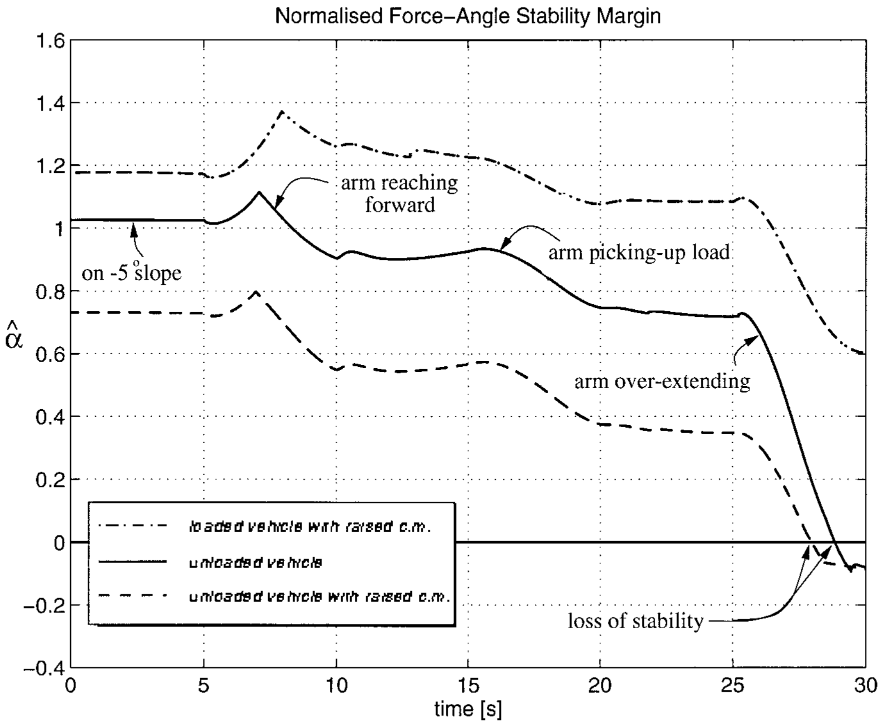

Fig. 7. Force-Angle stability measure for three cases of sample task.

lator joint angle and vehicle pitch angle time histories are presented in Figure 8, and the prescribed end-effector tip load time history is presented in Figure 9.

In Figure 7 it can be seen that the initial normalized stability margin measure is greater than one. This is due to the fact that system C.M. is closer to the rear wheel and the initial primary tipover axis candidate is the rear axis, (i.e., θ of Eq. (16) is minimum for the rear axis, $i = 2$, as can be seen in Table 1.) The tilt of the downwards slope moves the net force vector $\boldsymbol{f}_r$ towards the middle of the two tipover axes, away from the rear tipover axis, and the vehicle stability margin is improved. When the manipulator is commanded to reach forward (from $t = 5$ s to $t = 10$ s), the system C.M. consequentially moves forward and the stabilizing moment on the vehicle also increases. The result is thus an increase in the Force-Angle stability margin until the optimal Force-Angle is achieved and the stability margin reaches a peak. At this point, the principal tipover axis switches from the rear axis to the front axis. As the arm continues to reach forward, the tipover stability margin is progressively reduced as system C.M. motion and the effective moment on the vehicle are destabilizing. When the arm picks up the tip load of 750 kg (from $t = 15$ s to $t = 20$ s) we see a further important reduction in the tipover stability margin. If the base is not displaced and the arm is used to

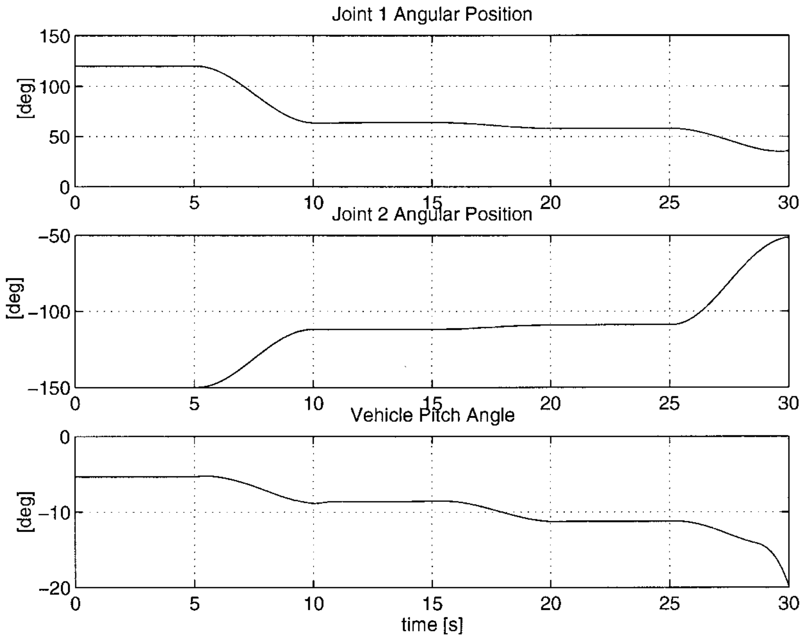

Fig. 8. Joint angles and vehicle pitch for sample task (case A).

move the load forward (from $t = 25$ s to $t = 30$ s), the tipover stability margin goes to zero and becomes negative as the vehicle tips forward.

By monitoring the Force-Angle stability margin an operator or an autonomous system could have avoided tipover by adopting a more suitable technique for displacing the load forward, such as by moving it closer to the vehicle with the manipulator and using simultaneous or subsequent forward motion of the platform.

For case B, where the vehicle has an initial load and its center-of-mass is raised, we see in Figure 7 that the effect of the increased heaviness is more important than the effect of the raised center-of-mass as the tipover stability margin is increased rather than decreased. The increased stability due to the

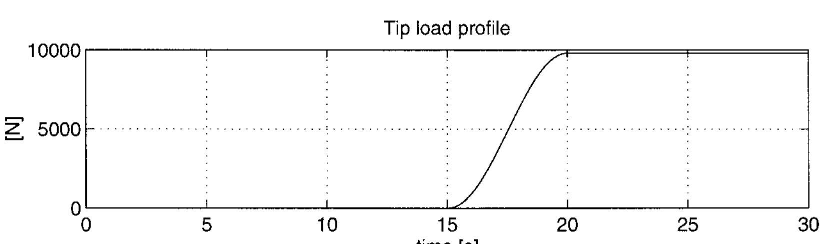

Fig. 9. Tip load profile for all cases of sample task.

increased mass of the base is sufficient in fact to prevent the tipover instability from occurring at the end of the tip load displacement. For case C, where the vehicle has a raised center-of-mass without an associated increase in mass, the Force-Angle tipover stability measure is reduced and, as expected, the tipover instability occurs sooner than for the other more stable cases.

7. COMPARISON WITH OTHER STABILITY MARGIN MEASURES

To better highlight the difference in performance expected between the Force-Angle measure and measures which are not sensitive to changes in center-of-mass height we computed the performance of five different stability margin measures for an unloaded vehicle performing the sample task of Section 5 with and without a raised center-of-mass (i.e., cases A and C). The stability margin measures computed were the static stability margin measure of McGhee et al. [7,8], the dynamic stability margin measure of Sreenivasan et al. [11], the virtual power stability measure of Davidson et al. [12], and the energy stability level measure of Messuri et al. [13] as extended by Ghasempoor et al. [14], and the Force-Angle

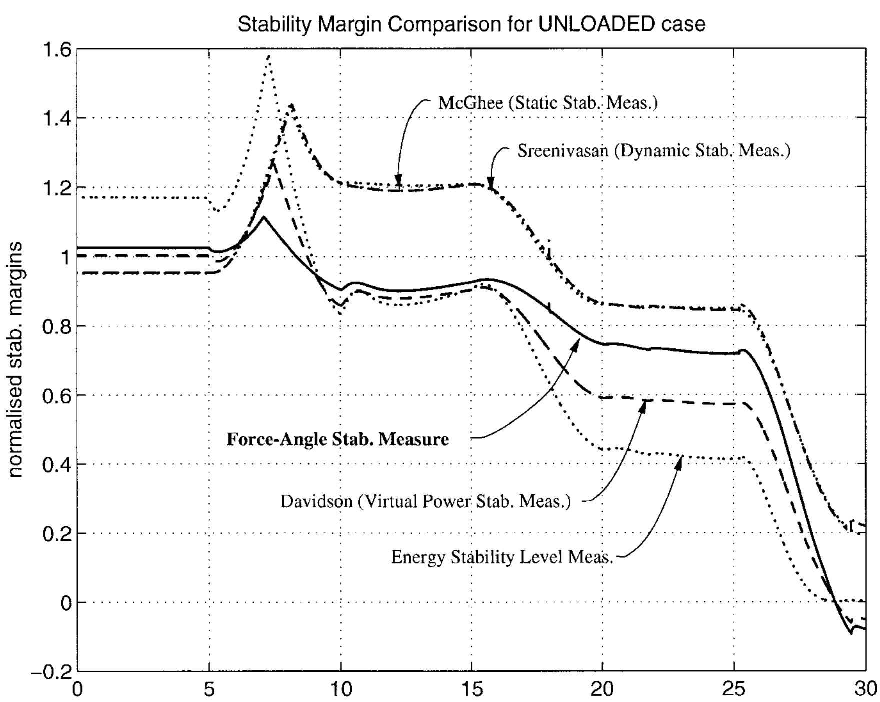

Fig. 10. Comparison of stability margin measures for unloaded system (case A).

proposed herein. Sreenivasan's measure was enhanced to include manipulator inertial forces and end-effector forces. Ghasempoor's measure was enhanced to include vehicle inertial forces and moments.

In order to simplify the comparison, all measures were normalized with respect to their nominal value for the mobile manipulator in its nominal configuration on a level surface. As can be seen in Figure 10 and Figure 11 all measures have the same general form. Closer inspection reveals a number of important observations. First, inertial effects are not very important for this slow moving system as McGhee and Sreenivasan's measure are nearly identical. By comparing the zero intercept of these measures to that of the other measures we observe that both of these measures are ineffective in predicting the onset of tipover. This is due to the fact that they are insensitive to angular loads. Next we note that the two energy based measures yield comparable results to the Force-Angle measure for the nominal center-of-mass height case of Figure 10. However, comparing this figure to that of Figure 11, we see that only the Force-Angle stability measure and the Energy stability measure are sensitive to the reduced stability of the system due to the raised center-of-mass. They are thus the only two comprehensive stability margin measures proposed to date. In the vicinity of the tipover onset we can also note that Force-Angle stability measure and Virtual Power stability measure are

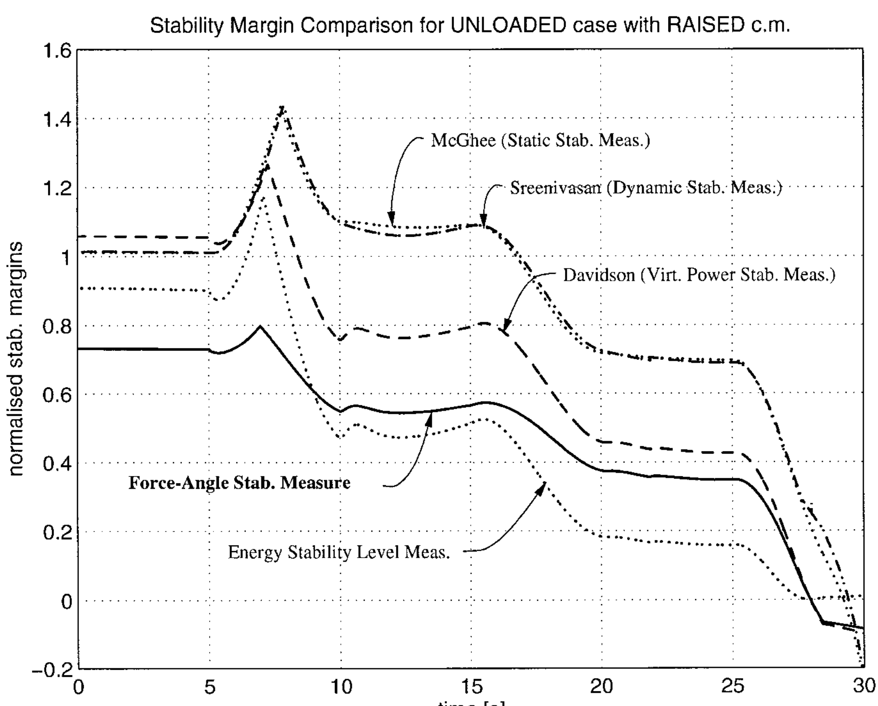

Fig. 11. Comparison of stability margin measures for unloaded system with raised C.M. (case C).

better behaved than the Energy stability measure which approaches the point of critical stability in an asymptotic fashion (making its gradient an unsuitable measure for an automated tipover prevention or recovery procedure).

8. COMPUTATIONAL REQUIREMENTS

Since all measures are linear, non-recursive methods, which largely require computation of the same system variables, the difference in computational cost between them is not large. However, for a real-time implementation these differences can become important (particularly if a control loop makes use of the stability margin measure). As a reference for suitability to real-time implementation, the Force-Angle stability margin measure computation was found to require 0.069 ms on an R4400, 150/75 MHz processor. Computationally, the main difference between the Force-Angle measure and the Energy measure is that the latter requires the computation of equilibrium planes for each tipover axis which is not needed in computing the Force-Angle measure.

9. CONCLUSIONS

This work presented a simple new measure of the tipover stability margin for mobile vehicles or mobile manipulators operating on arbitrarily uneven terrain: the Force-Angle stability margin measure. Applications of the simple criterion include tipover prediction and prevention in a real-time monitoring application, and off-line optimization for a trajectory planning or system design application.

Computation of the criterion only requires knowledge of the system mass properties and manipulator joint angles to compute the center-of-mass position, knowledge of the reaction loads at the system support points to compute the net force acting on the system C.M., and knowledge of the ground contact positions relative to the system C.M. to compute the tipover mode axes. The simple criterion can then be computed based principally on the minimum angle between the effective net force and the tipover axis normals. In addition to being relatively simple to interpret, compute, and implement, the Force-Angle measure has the important advantages of being sensitive to topheaviness and applicable to mobile manipulators subject to inertial loads and external forces of any kind. As all destabilizing influences are considered and the measure is applicable over uneven terrain, it can be said to be the only comprehensive measure of the tipover stability margin.

Performance of the measure and its proposed normalization was demonstrated using a forestry vehicle simulation for various vehicle loading and center-of-mass height initial conditions. The importance of being sensitive to changes in center-of-mass height and to changes in system heaviness was also highlighted with this example. Finally, performance of the Force-Angle stability measure was compared against that of several other fundamental stability margin measures proposed to date and was found to yield equivalent or better results despite its simple nature.

While the Force-Angle measure can already be used as-is in a number of important applications, future research is needed to investigate how best to exploit the measure in solving the problem of tipover prevention and recovery for mobile manipulators.

ACKNOWLEDGEMENTS

The support of this work by the IRIS-2 Centres of Excellence (ISDE-4) and by the Fonds pour la Formation de Chercheurs et l'Aide à la Recherche (FCAR) is gratefully acknowledged.

REFERENCES

1. Jones, I.S., and Penny, M.B. ''Engineering parameters related to rollover frequency'', *SAE Trans.*, 900104, 1990.
2. Buchele, W., and Xie, L. ''Computer analysis of the lateral stability of agricultural tractors'', *Proc. Amer. Society of Agricultural Eng. Winter Meeting*, no. 901589, 1990.
3. Blakenship, J.W., Means, K.H., and Biller, C.J. ''Side slopes static stability of double-articulated logging tractor'', *SAE Trans.*, no. 841140, 1984.
4. Li, Y., and Frank, A.A. A moving base robot, *Proc. American Control Conference*, Seattle, WA, pp. 1927–1932, June 1986.
5. Dubowsky, S., and Vance, E.E. Planning mobile manipulator motions considering vehicle dynamic stability constraints, *Proc. IEEE Int. Conf. on Robotics and Automation*, (Scottsdale, A.Z.), pp. 1271–1276, May 1989.
6. Shiller, Z., and Gwo, Y.-R. Dynamic motion planning of autonomous vehicles. *IEEE Trans. on Robotics and Automation*, 7, pp. 241–249, Apr. 1991.
7. McGhee, R.B., and Frank, A.A. On the stability properties of quadruped creeping gait. *Mathematical Biosciences*, 3 (2) pp. 331–351, 1968.
8. McGhee, R.B., and Iswandhi, G.I. Adaptive locomotion of a multilegged robot over rough terrain. *IEEE Trans. on Systems, Man, and Cybernetics*, SMC-9 (4), pp. 176–182, 1979.
9. Song, S.M., and Waldron, K. *Machines that Walk*. Cambridge, MA. MIT Press, 1989.
10. Sugano, S., Huang, Q., and Kato, I. Stability criteria in controlling mobile robotic systems, *Proc. IEEE/RSJ Int. Workshop on Intelligent Robots and Systems*, (Yokohama, Japan), pp. 832–838, July 1993.
11. Sreenivasan, S.V., and Wilcox, B.H. Stability and traction control of an actively actuated micro-rover. *J. of Robotic Systems*, 11, pp. 487–502, Sept. 1994.
12. Davidson, J.K., and Schweitzer, G. A mechanics-based computer algorithm for displaying the margin of static stability in four-legged vehicles. *Trans. ASME J. Mechanical Design*, 112, pp. 480–487, Dec. 1990.
13. Messuri, D.A., and Klein, C.A. ''Automatic body regulation for maintaining stability of a legged vehicle during rough-terrain locomotion'', *IEEE J. Robotics and Automation*, RA-1, pp. 132–141, Sept. 1985.
14. Ghasempoor, A., and Sepehri, N. A measure of machine stability for moving base manipulators, *Proc. IEEE Int. Conf. on Robotics and Automation*, (Nagoya, Japan), pp. 2249–2254, May 1995.
15. Papadopoulos, E.G., and Rey, D.A. A new measure of tipover stability margin for mobile manipulators, *Proc. IEEE Int. Conf. on Robotics and Automation*, (Minneapolis, MN), April 1996.
16. Karnopp, D. Computer simulation of slip-stick friction in mechanical dynamic systems. *Trans. ASME J. Dynamic Systems, Measurement, and Control*, 107, pp. 100–103, 1985.
17. Haessig, J.D.A., and Friedland, B. On the modeling and simulation of friction. *Trans. ASME J. Dynamic Systems, Measurement, and Control*, 113, pp. 354–362, Sept. 1991.